ENVIRONMENTAL RESEARCH
LETTERS

LETTER • OPEN ACCESS

Importance of beginning industrial-era climate simulations in the eighteenth century

IOP Publishing Environ. Res. Lett. 21 (2026) 014022 https://doi.org/10.1088/1748-9326/ae1bbc

ENVIRONMENTAL RESEARCH
LETTERS

LETTER

Importance of beginning industrial-era climate simulations in the eighteenth century

Andrew P Ballinger[1], Andrew P Schurer[1,*], Gabriele C Hegerl[1], Andrea J Dittus[2], Ed Hawkins[2], Richard Cornes[3], Elizabeth C Kent[3], Lauren R Marshall[4,7], Colin P Morice[5], Timothy J Osborn[6], Nick A Rayner[5] and Steven T Rumbold[2]

[1] School of GeoSciences, University of Edinburgh, Edinburgh, Scotland, United Kingdom
[2] National Centre for Atmospheric Science and Department of Meteorology, University of Reading, Reading, United Kingdom
[3] National Oceanography Centre, Southampton, United Kingdom
[4] Department of Earth Sciences, Durham University, Durham, United Kingdom
[5] Met Office Hadley Centre, Exeter, United Kingdom
[6] Climatic Research Unit, School of Environmental Sciences, University of East Anglia, Norwich, United Kingdom
[7] Now at: School of Earth and Environmental Sciences, University of St Andrews, St Andrews, Scotland, United Kingdom.
[*] Author to whom any correspondence should be addressed.

E-mail: a.schurer@ed.ac.uk

OPEN ACCESS

RECEIVED
2 April 2025

REVISED
15 August 2025

ACCEPTED FOR PUBLICATION
5 November 2025

PUBLISHED
6 January 2026

Keywords: early industrial period climate, climate variability, Earth system models, volcanic forcing

Supplementary material for this article is available online

Abstract

Climate simulations of the industrial era typically start in 1850, using the first fifty years as a baseline for 'pre-industrial' climate. However, the period immediately prior to 1850 is of particular interest due to early human influence and heightened volcanic activity, the latter of which led to cooler global temperatures than those observed in the subsequent historical period. In this study, we present a suite of Earth system model simulations (using UKESM1.1) that start in 1750 and span the entire industrial period. We compare these simulations to a new instrumental observation-based dataset, GloSATref, which provides global surface air temperature variations from 1781 onwards. We investigate the climatic changes during the early industrial period, separating the effects of natural and anthropogenic forcings. Model-simulated early-19th-century temperature patterns show substantial cooling relative to the long-term mean, particularly in low latitudes, which agree well with observed patterns. We find significant long-term differences between simulations initialized in 1750 and 1850, with lasting effects well into the 20th century, consistent with differences in vegetation and the substantial ocean cooling driven by high volcanic activity in the 1750 simulations. Our results indicate that an earlier start to historical simulations could lead to more representative climate simulations over the historical period, and deepen our understanding of early anthropogenic warming, natural climate variability, and the climate responses to future volcanic eruptions.

1. Introduction

Over the past few decades, substantial resources have been dedicated to generating model simulations of the past, which can be compared to observed changes in climate. Most simulations are run over the so-called 'historical' period, typically covering the period from 1850 to the present (Taylor *et al* 2012, Eyring *et al* 2016). These simulations have been widely used in various analyses to evaluate climate models and understand the causes of past climate changes (Bindoff *et al* 2014, Eyring *et al* 2021). The choice to start in 1850 is pragmatic, as it marks the period when instrumental surface temperature observations became more widely available.

However, it has long been realized that there was likely an earlier human influence from fossil fuel burning and land-use change, which produced greenhouse gas emissions and caused significant changes to albedo and other surface characteristics

(Tett *et al* 2007, Lamarque *et al* 2010, Schurer *et al* 2013, Abram *et al* 2016). The amount of global warming from a pre-industrial state is particularly significant, as it serves as the baseline for the UNFCCC to assess global temperature changes and set internationally agreed goals (Schleussner *et al* 2016). Due to the start dates of observational datasets and model simulations, the pre-industrial period has typically been represented by the late 19th century. This choice was supported by the Sixth Assessment Report (AR6) of the Intergovernmental Panel on Climate Change (IPCC), which used 1850–1900 as an approximate baseline from which changes from the pre-industrial period were expressed (Chen *et al* 2021). However, the IPCC also estimated that anthropogenic warming before this period was between 0.0 °C and 0.2 °C (Chen *et al* 2021). This estimate was based on various lines of evidence, including instrumental observations, forcing information, and model simulations, as discussed in Hawkins *et al* (2017) and Schurer *et al* (2017). Nonetheless, the exact value remains uncertain, and the IPCC only assessed this range with medium confidence. Thus, new lines of evidence are still needed.

To complement the historical model experiments, other simulations have been run covering periods further back in time, often under the framework of the Paleoclimate Modelling Intercomparison Project (PMIP; e.g. Braconnot *et al* 2012, Kageyama *et al* 2018). These include simulations covering the entire last millennium (Schmidt *et al* 2012, Jungclaus *et al* 2017), which have primarily focused on understanding pre-industrial changes caused by natural forcings and internal variability. This has ensured that there is a community-agreed, common set of boundary conditions for the entire last 2000 years, which are available to run climate simulations of this period. Analyses of these PMIP simulations have highlighted the important role of volcanic eruptions in the climate of this period (Schurer *et al* 2014, Otto-Bliesner *et al* 2016), which caused periods of global surface cooling and long-term changes to ocean temperature (Gleckler *et al* 2006), sea ice (Miller *et al* 2012), and modes of variability such as the Atlantic meridional overturning circulation (AMOC; Pausata *et al* 2015, Swingedouw *et al* 2017).

One of the coldest periods of the last millennium occurred in the early 19th century, caused by several large volcanic eruptions, most notably Mount Tambora in 1815 (PAGES2K 2013, Raible *et al* 2016, Brönnimann *et al* 2019b). This period of volcanism was much stronger than anything in the subsequent historical period. The historical experiments, typically beginning in 1850, thus miss an important opportunity to study this volcanically active period and potentially introduce biases by neglecting its long-term effects (e.g. Gregory *et al* 2013). Examining this era could enhance our understanding of Earth system responses and better prepare us for the potential climate effects of future volcanic eruptions.

Although some instrumental observations extend back to the 17th century (e.g. HadCET; Parker *et al* 1992), existing observation-based, globally gridded datasets of surface temperature begin in 1850 or later (Gulev *et al* 2021), limited by the availability of sea surface temperature (SST) measurements, which are blended with air temperature measurements over land and ice to create the global record. Recently, a new dataset, **GloSATref** (Morice *et al* 2025), has been constructed by the UK Global surface air temperature (GloSAT) project. It combines marine air temperatures with land station data to extend the observed period back to the late 18th century.

Here we present new simulations starting in 1750 using UKESM1.1, a state-of-the-art Earth System Model (Mulcahy *et al* 2023), which is suitable to explore the implications of extending the historical period back into the 18th century. In the next section, we will introduce the UKESM1.1 model configuration and experiment simulations (section 2.1), along with the GloSATref observational dataset (section 2.2). We will then present our results (section 3), analyzing the new control and historical simulations, and comparing them with the new observational dataset. Finally, we will discuss our findings more broadly, offering suggestions for how the community might further explore some of the questions raised (section 4).

2. Model Simulations and Observational Dataset

2.1. UKESM1.1 simulations

The climate model used in this study is UKESM1.1, an updated configuration of the UKESM1.0 climate model described in Sellar *et al* (2019, 2020). UKESM1.1 is the UK's state-of-the-art Earth system model, which integrates an atmosphere-land-ocean-sea ice model with terrestrial and ocean biogeochemistry, and a comprehensive aerosol and chemistry scheme. UKESM1.1 builds on UKESM1.0 with several modifications, including improvements to the dry-deposition scheme (Hardacre *et al* 2021) that reduce a known bias in aerosol forcing (Dittus *et al* 2020, Mulcahy *et al* 2020) as discussed in Mulcahy *et al* (2023). UKESM1.1 has been used to run the standard suite of CMIP6 experiments, including the Diagnostic, Evaluation and Characterization of Klima experiments (Eyring *et al* 2016). For this study, we focus on a standard pre-industrial control (piControl) simulation with constant 1850 forcing, and an ensemble of six historical simulations (1850–2014) initialized from the piControl experiment (historical). UKESM1.1 has a relatively high climate sensitivity, with an effective climate sensitivity of 5.27 K and a transient climate response of 2.64 K (Mulcahy

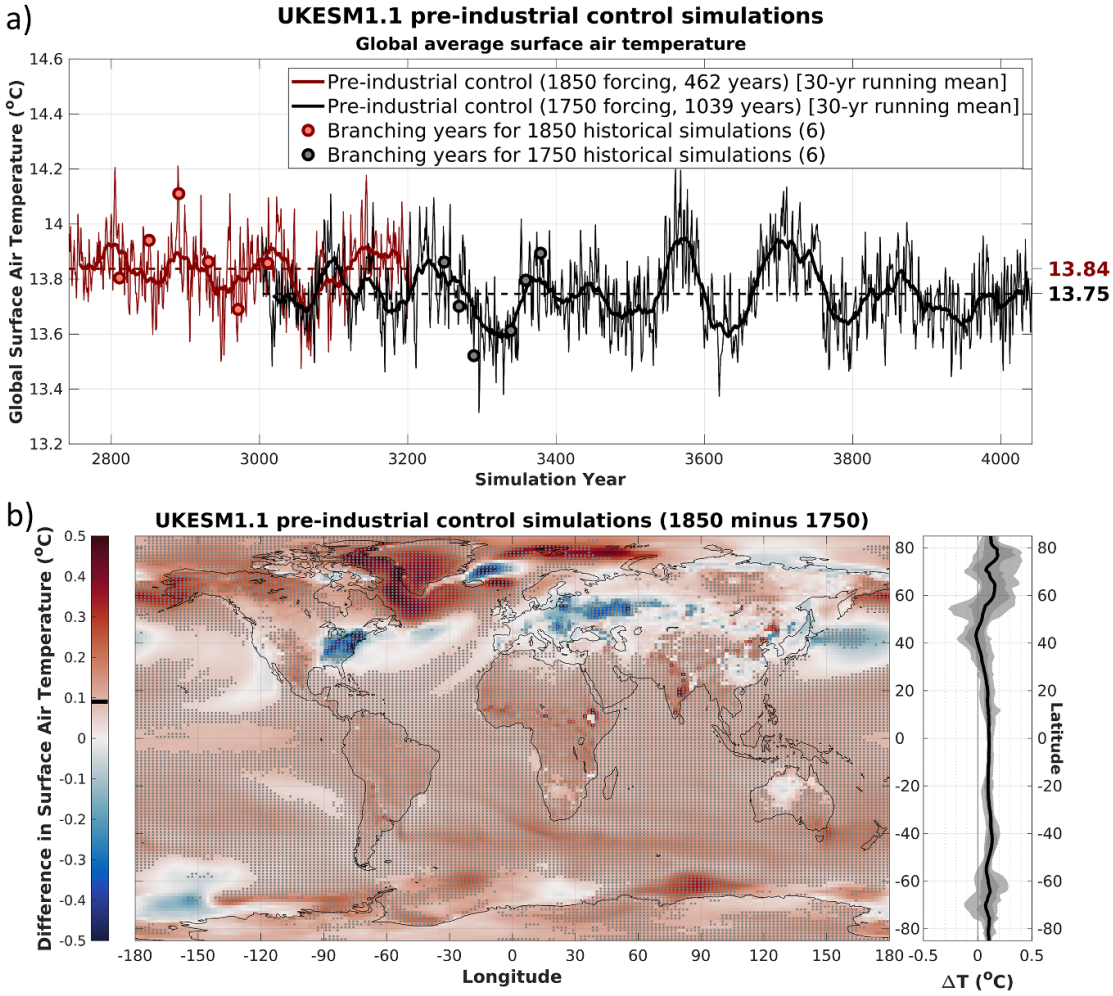

Figure 1. (a) Global mean surface air temperature (GSAT, °C) for the UKESM1.1 piControl simulations, with constant forcing at 1750 (black) and 1850 (red; see Mulcahy *et al* 2023) values, showing interannual variability (thin lines) and the 30 yr running mean (thick lines). Horizontal dashed lines show the control simulation GSAT means of 13.75 °C and 13.84 °C, respectively. Circle markers indicate the control simulation years from which the subsequent historical simulations are initiated (see section 2.1.2). (b) Map of the difference in SAT between the $piControl_{1850}$ and $piControl_{1750}$ simulations, with stippling indicating significance (via two-sample K–S test at the 5% level). The right-hand panel shows the zonal means of the control run differences in SAT, with the ensemble mean in black and the spread in grey.

et al 2023). The additional model simulations analysed in this study are described below (sections 2.1.1 and 2.1.2) and summarized in the supplementary table S1.

2.1.1. 1750 piControl simulation

To initialize our transient simulations in 1750, a 'spin-down' simulation was performed to provide initial conditions in equilibrium with the 1750 climate. This simulation is analogous to the standard piControl simulation, which serves as the starting point for historical simulations from 1850. The spindown simulation branched from the standard piControl but held anthropogenic forcings constant at 1750 values (where available).

Specifically, the forcings modified were anthropogenic aerosol emissions (Hoesly *et al* 2018), greenhouse gas concentrations (Meinshausen *et al* 2017), and the extent of land used for agriculture, which was also set to 1750 values (Hurtt *et al* 2020), with the remaining land area controlled by the dynamic vegetation scheme (TRIFFID). As no CMIP6 values were available for ozone and nitrogen deposition, these were held constant at the 1850 values. Natural forcings (volcanic and solar) were identical to the long-term average values used in the 1850 piControl, as specified in Eyring *et al* (2016). Therefore, the only difference between the two control simulations was the difference in anthropogenic forcings between 1750 and 1850. We refer to this new simulation as $piControl_{1750}$ and the standard piControl as $piControl_{1850}$ for clarity.

2.1.2. Historical simulations (1750–2014)

Six historical all-forcing simulations spanning the period 1750–2014 were spawned from the $piControl_{1750}$ simulation, branching at regular intervals as indicated in figure 1(a). For the period 1750–1849, the forcings mainly follow those recommended for the CMIP6 past1000 experiment (Jungclaus *et al*

2017), including volcanic (Toohey and Sigl 2017), solar (the ^{14}C SATIRE-based reconstruction: Vieira *et al* 2011, Wu *et al* 2017), greenhouse gas emissions (Meinshausen *et al* 2017) and land-use changes (Hurtt *et al* 2020). In the CMIP6 past1000 simulations, anthropogenic aerosols were kept at constant 1850 values, but in our setup, we use time-varying values from the dataset used for CMIP6 historical simulations, extending back to 1750 (Hoesly *et al* 2018). This approach closely follows that of Marshall *et al* (2024), although we implement volcanic forcing using aerosol optical property concentrations, as described in Sellar *et al* (2019), rather than volcanic emissions.

For the period after 1850, the simulations use the same forcings to the CMIP6 historical simulations (1850–2014) described in Mulcahy *et al* (2023). Consequently, the only difference between the two sets of simulations lies in their initial conditions. Our new experiments are referred to as historical$_{1750}$ to distinguish them from the standard historical simulations, which are referred to as historical$_{1850}$.

To isolate the impact of natural forcing during the early industrial period—dominated by volcanic eruptions and a small contribution from solar variability (Schurer *et al* 2014, Jungclaus *et al* 2017) — four additional simulations were started from the same initial conditions as the first four historical$_{1750}$ simulations. In these simulations, referred to as historicalANT$_{1750}$, the natural forcings are held constant at piControl values from 1750–1850, while after 1850 the forcings are identical to those in the historical$_{1850}$ simulations. Thus, any differences from the historical simulations will be solely due to the absence of natural forcing variability between 1750–1850.

2.2. GloSATref observational dataset

Although gridded global temperature datasets are typically limited to start in 1850 due to the availability of SST observations, earlier records of air temperature from ships (Freeman *et al* 2017) and land-based observations (Brönnimann *et al* 2019a) exist. However, these early observations are sparse, and constructing a homogeneous surface air temperature (SAT) record presents several challenges (Kent and Kennedy 2021, Wallis *et al* 2024). The GloSATref dataset (Morice *et al* 2025) is the first to combine land and ocean air temperature observations. It uses the analysis methods used by Morice *et al* (2021) for the HadCRUT5 Analysis dataset, with a Gaussian process model extending the coverage to also provide temperature anomalies for those grid cells that do not contain an observation, but for which available observations from further afield are informative. It extends the SAT record back to the 1780s, although the early part of the record has substantial uncertainty and limited geographical coverage. Comparisons between GloSATref and existing SST-based datasets for global mean temperature show broad consistency, with some differences. Notably, from 1885–1915 GloSATref is consistently cooler than the other datasets, and after 1950 the warming trend in GloSATref is slightly lower than in the SST-based datasets (Morice *et al* 2025).

3. Results

3.1. Comparing the 1750 and 1850 piControl climatologies

The only difference between the two piControl simulations (the existing piControl$_{1850}$ and the new simulation piControl$_{1750}$) is the change in anthropogenic forcings between these dates (see section 2.1.1, table S1). Since the period around 1750 has been suggested as a good approximation for a true pre-industrial climate (Hawkins *et al* 2017), the difference in climate between the two simulations should reflect the early anthropogenic effect before 1850. Given the lengths of the two simulations (461 years and over 1000 years, respectively), we can calculate a precise global-mean SAT (GSAT) increase of 0.09 °C by averaging over the full simulation periods (figure 1(a)). The GSAT is also 0.09 °C higher than piControl$_{1750}$ in the 1850–1900 mean calculated from the average of the six historical$_{1750}$ ensemble members. Assuming piControl$_{1750}$ represents a 'true' pre-industrial climate, this provides an estimate of the early industrial warming, typically overlooked when using the 1850–1900 mean.

The spatial pattern of this difference (figure 1(b)) shows that the early anthropogenic effect caused warming for much of the globe, but this is not the case everywhere. Notable exceptions include the eastern parts of North America, much of Europe, and East Asia. In these regions, pronounced simulated vegetation changes occurred during this period (see Supplementary figures S5–S11), with natural vegetation converted into agricultural land, including crops (figure S5(b)) and pasture (figure S6(b)). This pattern is consistent with a previous study by Boysen *et al* (2020), which investigated the effect of deforestation in CMIP6 models, finding that deforestation of boreal regions causes a zonal mean cooling in the extratropics around 40 °N, primarily due to changes in albedo. This result was observed in the majority of models they investigated, including UKESM, and the pattern closely matches that shown in figure 1(b).

In contrast, parts of India that have undergone the greatest vegetation changes show slightly more warming than the global mean, consistent with model simulations that suggest deforestation in tropical regions can cause warming due to changes in evapotranspiration (Claussen *et al* 2001). Additionally, there is likely an effect from the early increase in anthropogenic aerosols, which may have contributed to some

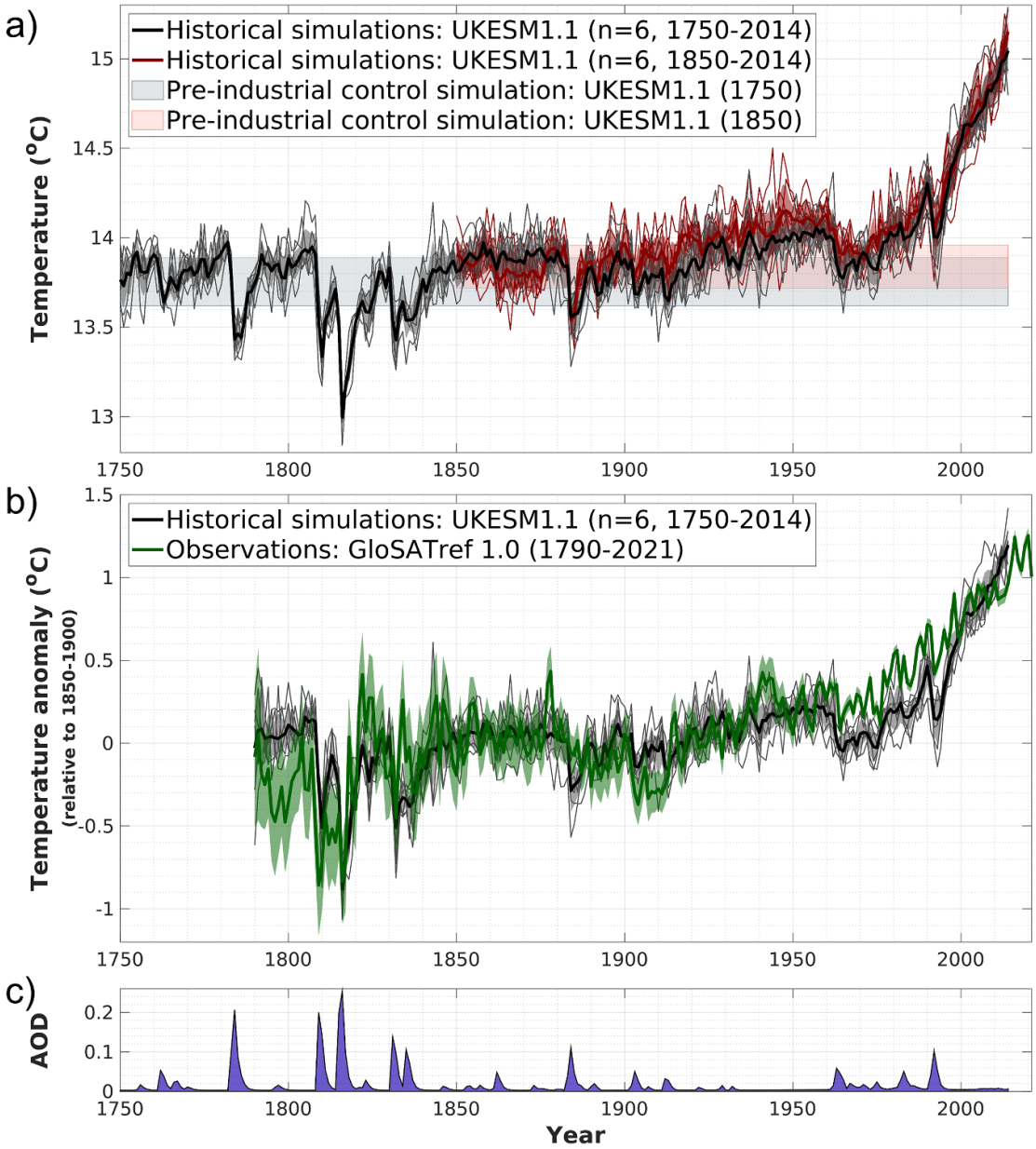

Figure 2. Annual global mean surface air temperature, shown for (a) the two sets of UKESM1.1 historical simulations, starting in 1750 (black) and 1850 (red; see Mulcahy *et al* 2023); and (b) the UKESM1.1 historical$_{1750}$ simulations (black) compared with the new GloSATref observational data (green), as anomalies referenced to 1850–1900, with the model simulations masked to the time-evolving observational coverage for 1790–2021. The individual UKESM1.1 model ensemble members (thin lines, six members per experiment) and the ensemble mean (thick lines) are shown, along with shaded confidence interval (2.5–97.5th percentile range). The shaded rectangles in (a) show the interannual spread (2.5–97.5th percentile range) of internal variability calculated from the associated piControl simulations. (c) Global mean stratospheric aerosol optical depth (Toohey and Sigl 2017).

of the regional cooling simulated from 1750 to 1850 (Carslaw *et al* 2017). The northern Arctic regions show more warming than the global mean, possibly due to Arctic amplification, sea ice loss and a slightly strengthened AMOC (figure S17).

3.2. The transient historical simulations

The evolution of GSAT in the historical$_{1750}$ simulations is shown in figure 2(a). A striking feature is the large cooling during the early 19th century, with the ensemble mean GSAT lower than the 1850–1900 mean for much of the period from 1810 to the mid-1840s. This cooling is due to a series of large volcanic eruptions in 1808–9 (unknown), 1815 (Tambora), 1822 (Galanggung), 1831 (uncertain) and 1835 (Cosiguina) (Schurer *et al* 2014, Raible *et al* 2016, Brönnimann *et al* 2019b). The volcanic activity is reflected in the time series of global stratospheric aerosol optical depth (AOD) shown in figure 2(c). This substantial cooling is also seen in the GloSATref observational dataset (figure 2(b); green), with the coolest temperatures corresponding to the volcanic periods of the 1810s and 1830s. Previous studies (Brohan *et al* 2012, Schurer *et al* 2013) have generally found that model simulations overestimate the cooling compared to sparse instrumental observations or

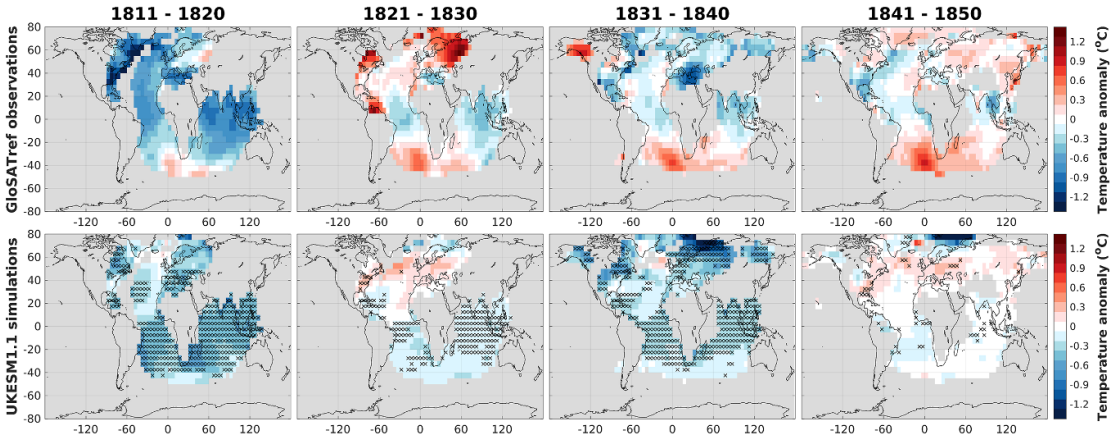

Figure 3. Decadal mean surface air temperature anomalies from the GloSATref observational dataset (top row; 1811–1820, 1821–1830, 1831–1840 & 1841–1850), and the UKESM1.1 model ensemble mean of the six historical$_{1750}$ simulations for the same decades (bottom row), plotted relative to the 1850–1900 climatology. Model simulations have been masked to the observational coverage, and the grid boxes with crosses show where the decadal mean anomaly from all six ensemble members agree with the sign of the ensemble mean.

proxy reconstructions. It is therefore notable that the cooling in the historical$_{1750}$ simulations is in better agreement with this new observational dataset.

In figure 2(b), the model data (black) is first masked to the observational coverage, enabling a consistent comparison. An evaluation based on model simulations shows that, even though geographic coverage is severely limited in the early period, the available data still provide a reasonable estimate of the true global mean (figure S1). One noticeable exception to this occurs during the cooling caused by the Laki eruption of 1783. The impact of this eruption is concentrated in the northern extratropics (see e.g. Zambri *et al* 2019), where nearly all the observational data are located during this period. As a result, masking the model data to observational coverage accentuates the cooling. Additionally, because of the sparse observational coverage, variability around the mean (and hence the error in global mean estimates) increases further back in time.

Maps showing the spatial distribution of temperature anomalies for the key early decades (figure 3) reveal similar patterns in both the GloSATref observations and model simulations. Both indicate widespread cooler temperatures in the 1810s and 1830s, and relatively warmer temperatures in the 1820s and 1840s. The large areas of model agreement, where all 6 simulations have the same sign for decadal mean temperatures, highlight the key role that external forcing—particularly volcanic forcing—plays in these decades, dominating over the random influence of internal variability. All data are masked to observational coverage (note this is where observations are informative, even if not present in every grid cell; recall section 2.2), which, as figure 3 shows, is reasonably widespread even during this early period, covering much of the Atlantic and Indian Oceans, Europe, and by the 1840s, much of North America and Asia.

The standard historical$_{1850}$ simulations initialized in 1850 from piControl$_{1850}$ (see figure 1(a)) are also shown in figure 2(a). These simulations use the exact same model setup and forcings as our new simulations, so they might be expected to follow a similar evolution in GSAT over the common period. However, there are clear and statistically significant differences in the evolution of the two sets of experiments (figure S2), with the simulations initialized in 1750 showing better agreement with observed global mean surface temperature during parts of the late 19th and early 20th centuries (figures S3–S4). This, in addition to biases in observational datasets (Chan *et al* 2024, Sippel *et al* 2024), could potentially explain a long-standing discrepancy between model simulations and observational datasets during the early 20th century (Hegerl *et al* 2018). The mean difference in the early 20th century (1900–1930) far exceeds the 99th significance percentile (evaluated using samples from piControl), suggesting this difference originates from the initial conditions. Given the duration over which this difference persists, the most likely sources are components of the Earth system with the longest memory. Plausible candidates include land surface vegetation and heat stored in the ocean. Maps showing the spatial pattern for the difference during two periods, 1850–1880 and 1900–1930, are shown in figure 4.

The first 31-yr period (1850–1880, figure 4(a)) is cooler in the simulations initiated in 1850 than those initiated in 1750 ($p < 0.05$). This difference is particularly pronounced over Eastern Europe and the eastern US, regions with vegetation differences that persist from the piControl simulations they were initialized from. In these areas, the historical$_{1850}$

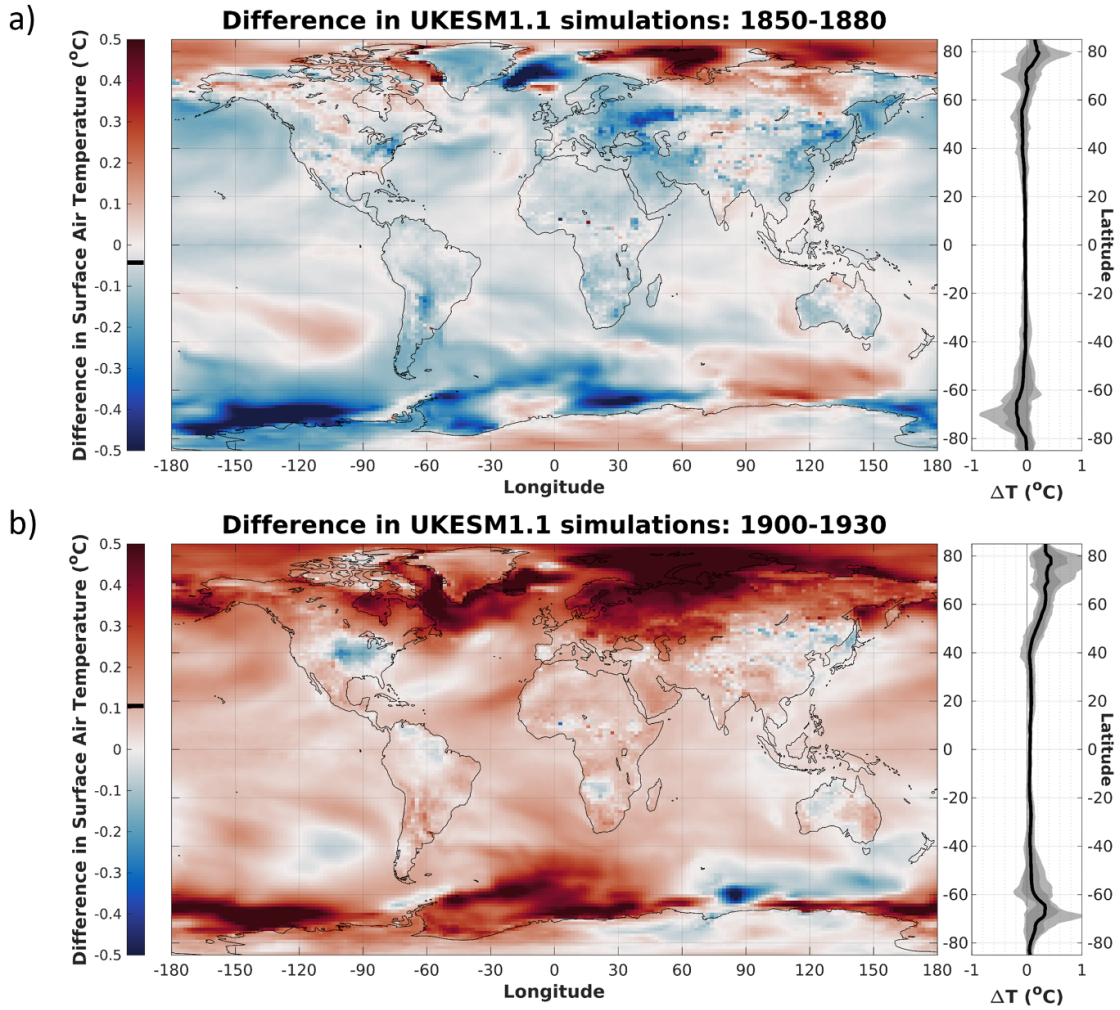

Figure 4. Difference in the annual global mean SAT, showing the UKESM1.1 historical$_{1850}$ simulations minus the new historical$_{1750}$ simulations, for the periods: (a) 1850–1880, and (b) 1900–1930. The right-hand panels show zonal means of the control run differences in SAT, ensemble mean in black and spread grey.

simulations show more grass (figure S7), whereas the historical$_{1750}$ simulations have more trees (figures S8–S9). A noticeable difference in vegetation is also observed across the high Arctic regions, with more shrubs (figure S10) and less bare soil (figure S11) in the historical$_{1850}$ simulations. These differences could at least partly explain the observed pattern (figure 4(a)). In the second 31 yr period (1900–1930, figure 4(b)), the historical$_{1850}$ simulations are warmer than the historical$_{1750}$ simulations ($p < 0.01$), with warmer conditions simulated across the majority of the globe. The pattern observed in this period is distinctly different from that in the 19th century, suggesting that the source of the difference likely differs from that of the earlier period.

Changes in ocean heat content due to pre-1850 natural forcing are shown in figure 5, highlighting the long-term impact of the series of volcanic eruptions in the early 19th century. Significant cooling is experienced throughout the upper and lower layers of the ocean, with some impacts persisting for decades. The cool anomaly descends through the ocean layers around Antarctica during the post-eruption period (figures S12–S13). The results in figure 5 suggest that the influence of pre-1850 volcanic forcing persists into the early 20th century and could, at least partly, explain the discrepancies observed in figures 4 and S1.

The historical$_{1750}$ simulations are substantially cooler throughout the middle and deep ocean relative to the piControl$_{1850}$ and historical$_{1850}$ simulations (figure S14). This highlights the importance of initial conditions, as the colder temperatures in the piControl$_{1750}$ simulation persist throughout the entire simulation. Figures S15 and S16 show that even after 800 yr, the ocean in the piControl$_{1750}$ simulation is still adjusting to the change in forcing from 1850 to 1750. Had we started from initial conditions where the entire ocean was in equilibrium, the volume-averaged ocean heat content would be lower, and

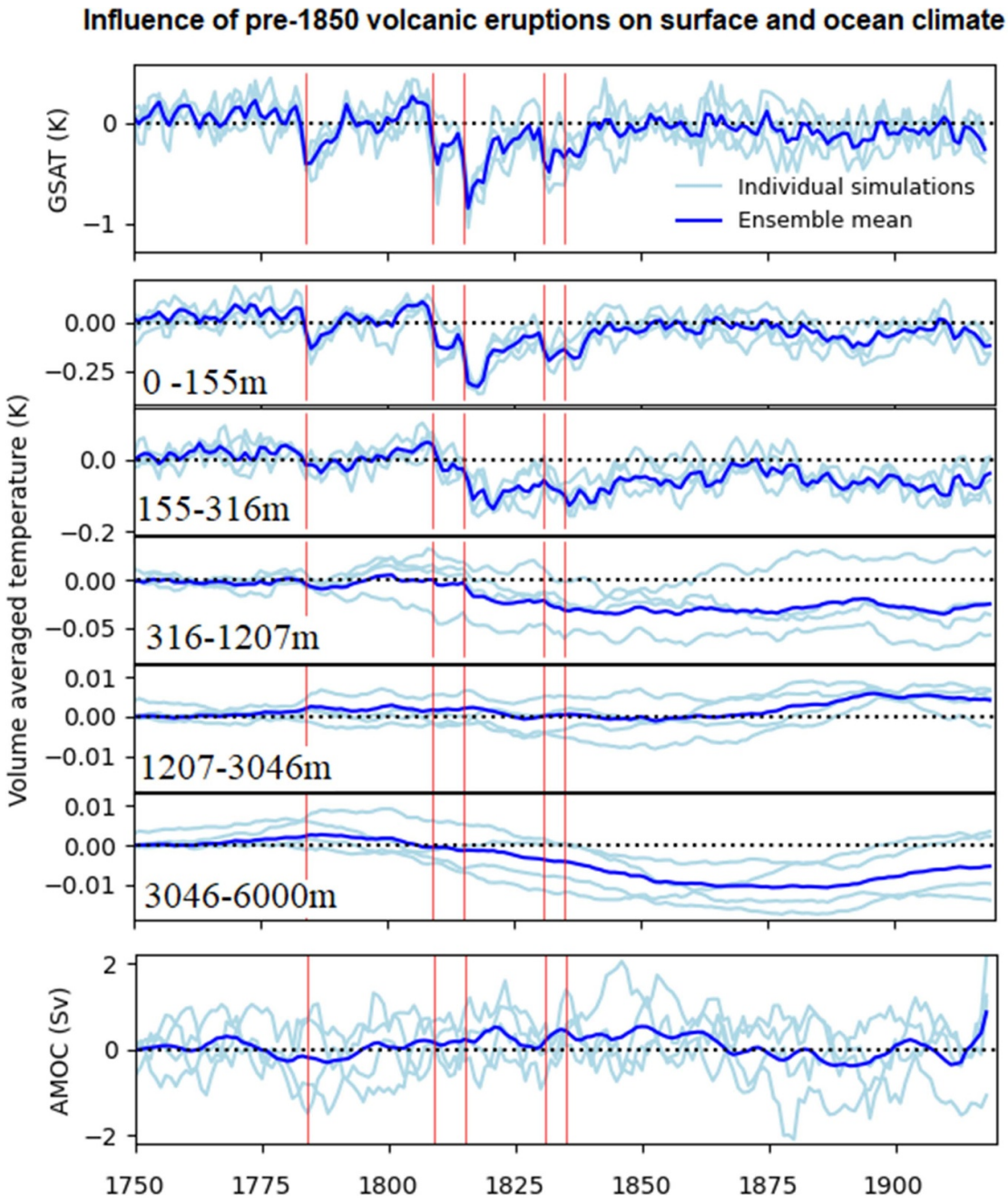

Figure 5. The effect of early natural forcing (1750–1850) on the ocean. Time series of the historical$_{1750}$ simulations minus historicalANT$_{1750}$ simulations, showing the difference in: the GSAT top panel); the ocean temperature anomaly at different depths (middle panels); and the AMOC, defined as the maximum meridional streamfunction in the Atlantic (bottom panel). Light blue lines depict individual ensemble members, and darker blue lines show the ensemble mean. The largest volcanoes during the 1750–1850 period are indicated by red vertical lines.

consequently, the differences in the deep ocean caused by the choice of starting year (shown in figure S14), would likely be even larger.

As suggested by previous studies (e.g. Pausata *et al* 2015, Swingedouw *et al* 2017), we also examine the effect of the volcanic eruptions on the AMOC. In agreement with Iwi *et al* (2012), we find a small increase in the AMOC following periods of strong volcanism, with the AMOC reaching a local maximum around 1840 (figure S18). The increasing trend from 1750 to the middle of the 19th century is highly significant ($p < 0.01$) when compared to equivalent samples taken at random from piControl$_{1750}$ (figures S19a and S19c). Therefore, at the start of the traditional 'historical' period, these results suggest that the AMOC is likely in a positive state (figure S19b), with implications for the subsequent climate. This finding is consistent with observed temperatures that show warmer conditions in the subpolar gyre region during much of the 19th century (Caesar *et al* 2018, Morice *et al* 2025). Comparisons with the historicalANT$_{1750}$ simulations suggest this

behavior can be linked to volcanic activity (figure 5), in agreement with Schurer *et al* (2023) who analyzed single-forcing simulations in an earlier version of the UK climate model (HadCM3).

4. Discussion and conclusions

Our transient simulations reinforce previous studies that have highlighted the significant impact of volcanic eruptions on the climate of the early 19th century, particularly in causing cooler conditions during the 1810s and 1830s (Hegerl *et al* 2019). We have also analyzed a new observational dataset that provides a broadly consistent picture of SAT changes during these decades, contrasting with earlier work that relied on sparser observational or proxy data and found less observed cooling than in simulations. Our analysis of ocean temperatures shows that cooling from these eruptions persisted well into the latter part of the 19th century and beyond, particularly in the deep ocean.

We find highly significant differences in surface climate between simulations initialized in 1750 and those initialized from a piControl simulation in equilibrium with 1850 conditions. Three key factors likely contribute to the memory of the initial conditions well into the 20th century. First, the ocean heat content differs based on the starting point—the ocean in equilibrium with 1750 is cooler than that in equilibrium with 1850—and this is compounded by cooling from large volcanic eruptions. These eruptions also affect ocean circulation through the AMOC, which could further influence the climate during the historical period. Lastly, initial vegetation differences between 1750 and 1850 continue to impact vegetation in our simulations throughout the 20th century.

Our results highlight potential issues with starting simulations from piControl simulations that assume the Earth system is in equilibrium with present conditions, when in reality, it is under constant change (Gregory *et al* 2013). Our findings, therefore, have implications for standard historical experiments, which typically start in 1850, as specified by CMIP. If the decision were made to start simulations 100 or even 50 yr earlier, this would lead to different—and potentially improved—simulations (see figures S3–S4), although further analysis using simulations from multiple climate models would be required to confirm this. If historical simulations are to start in 1850, an alternative approach to at least partially mitigate this issue could be to begin the simulations from initial conditions preferentially chosen to be cooler, with a relatively strong AMOC.

Further motivation for starting simulations at least 50 yr earlier is provided by the recent release of the GloSATref dataset, covering the period from 1781 onward. Understanding multi-decadal variability is crucial if we are to provide reliable projections of future climate. Studying past variability is an important component of this, best achieved by comparing observed and modeled climate. This period, therefore, presents an ideal opportunity to extend the available time period by approximately 40%. This is especially true for understanding multi-decadal Atlantic variability, which has reasonable early observational coverage (figure 3), and for which there is significant interest in the causes of changes (e.g. Zhang *et al* 2019). Equally important is the opportunity this period offers to study the effect of large volcanic eruptions, which we have found can influence the climate for many decades. These eruptions are, therefore, a vital aspect of the climate system to understand if we are to fully prepare society for the possibility of similar volcanic episodes occurring in the future (Bethke *et al* 2017).

The amount of anthropogenic warming that occurred before 1850 is still a contentious topic, with the IPCC estimating a range for pre-1850 anthropogenic warming with only medium confidence. In this study, we introduce a novel model setup involving two piControl simulations, which enables us to calculate this quantity with a high level of precision. The derived GSAT difference of 0.09 °C is consistent with the IPCC range [0.0 °C to +0.2 °C] for the anthropogenic component, lending confidence to their assessment. However, it is clear that this difference is not uniform (recall figure 1(b)), as the anthropogenic difference in SAT between 1750 and 1850 varies spatially, mainly due to vegetation changes. It is important to note that the climate represented by our piControl_{1750} does not correspond to any specific time period, since it does not account for changes in natural variability, which can lead to considerable climate differences even in the absence of human forcing (see Schurer *et al* 2017). Additionally, while 1750 is considered a good approximation of the pre-industrial climate (Hawkins *et al* 2017), anthropogenic land-use changes had already begun long before this date (e.g. Kaplan *et al* 2009, Malhi 2018, and also shown in figures S5–S6), suggesting that human influence on the climate was likely already underway.

In this article, we have highlighted the benefits of starting historical model simulations at least 50 yr earlier. Further simulations driven by single forcings or combinations of forcings would help disentangle the impact of different factors such as changes in land use, anthropogenic aerosols, greenhouse gases, and the effects of the initial conditions and model drift. Only one state-of-the-art Earth System Model has been used to perform these experiments to date, and we encourage others to consider similar approaches. Future modeling intercomparison projects may also consider preparing forcing files which extend back to 1750 as standard, so that these types of simulations can be more easily implemented. We would also recommend the development of a clear experimental protocol for extended historical simulations,

like those presented in this paper, to facilitate comparisons between results from different models.

Data availability statement

Data from the 6 historical 1750 ensembles members for a comprehensive number of monthly variables are available here: https://dx.doi.org/10.5285/9487085a6a3d4ca1aafa7c569e840d2a. All other new model variables and derived variables analysed in the paper are available here: https://dx.doi.org/10.5285/1d2b498e981f4bcfb46c1f3c5923b122.

Acknowledgment

This study was supported by the GloSAT project, funded by the National Environment Research Council (University of Edinburgh NE/S015698/1; NOC NE/S015647/2; University of Reading NE/S015574/1; University of East Anglia NE/S015582/1). In addition, A P S was funded by a University of Edinburgh Chancellor's Fellowship, A J D was funded by a NERC independent research fellowship (NE/X017850/1), and A P S, G C H and L M were funded by VolCLIM (NE/S000887/1). The authors are grateful for many helpful discussions, and for the people who have assisted in the setup of the model simulations, including: Alistair Sellar, Luke Abraham, Jane Mulcahy, Ben Johnson, Matt Toohey, Chris Jones, Eddy Robertson, Spencer Liddicoat, Harold Dyson, Mark Richardson, Jeremy Walton, Jared Drayton and the NCAS Computational Modeling Services team.

ORCID iDs

Andrew P Ballinger 0000-0003-3704-1976
Andrew P Schurer 0000-0002-9176-3622
Gabriele C Hegerl 0000-0002-4159-1295
Andrea J Dittus 0000-0001-9598-6869
Ed Hawkins 0000-0001-9477-3677
Richard Cornes 0000-0002-7688-4485
Elizabeth C Kent 0000-0002-6209-4247
Lauren R Marshall 0000-0003-1471-9481
Colin P Morice 0000-0002-5656-1021
Timothy J Osborn 0000-0001-8425-6799
Nick A Rayner 0000-0002-8334-5519
Steven T Rumbold 0000-0001-8138-4541

References

Abram N J, McGregor H V, Tierney J E, Evans M N, McKay N P and Kaufman D S 2016 Early onset of industrial-era warming across the oceans and continents *Nature* **536** 411–8

Bethke I, Outten S, Otterå O H, Hawkins E, Wagner S, Sigl M and Thorne P 2017 Potential volcanic impacts on future climate variability *Nat. Clim. Change* **7** 799–805

Bindoff N L *et al* 2014 Detection and attribution of climate change: from global to regional *Climate Change 2013: the Physical Science Basis* ed T F Stocker pp 867–952

Boysen L R *et al* 2020 Global climate response to idealized deforestation in CMIP6 models *Biogeosciences* **17** 5615–38

Braconnot P *et al* 2012 Evaluation of climate models using palaeoclimatic data *Nat. Clim. Change* **2** 417–24

Brohan P, Allan R, Freeman E, Wheeler D, Wilkinson C and Williamson F 2012 Constraining the temperature history of the past millennium using early instrumental observations *Clim. Past* **8** 1551–63

Brönnimann S *et al* 2019a Unlocking pre-1850 instrumental meteorological records: a global inventory *Bull. Am. Meteorol. Soc.* **100** ES389–ES413

Brönnimann S *et al* 2019b Last phase of the little ice age forced by volcanic eruptions *Nat. Geosci.* **12** 650–6

Caesar L, Rahmstorf S, Robinson A, Feulner G and Saba V 2018 Observed fingerprint of a weakening atlantic ocean overturning circulation *Nature* **556** 191–6

Carslaw K S, Gordon H, Hamilton D S, Johnson J S, Regayre L A, Yoshioka M and Pringle K J 2017 Aerosols in the pre-industrial atmosphere *Curr. Clim. Change Rep.* **3** 1–15

Chan D, Gebbie G and Huybers P 2024 An improved ensemble of land surface air temperatures since 1880 using revised pair-wise homogenization algorithms accounting for autocorrelation *J. Clim.* **37** 2325–45

Chen D *et al* 2021 Framing, context and methods *Climate Change 2021: The Physical Science Basis. Contribution of Working Group I to the Sixth Assessment Report of the Intergovernmental Panel on Climate Change* ed V Masson-Delmotte (Cambridge University Press) pp 147–286

Claussen M, Brovkin V and Ganopolski A 2001 Biogeophysical versus biogeochemical feedbacks of large-scale land cover change *Geophys. Res. Lett.* **28** 1011–4

Dittus A J, Hawkins E, Wilcox L J, Sutton R T, Smith C J, Andrews M B and Forster P M 2020 Sensitivity of historical climate simulations to uncertain aerosol forcing *Geophys. Res. Lett.* **47** e2019GL085806

Eyring V, Bony S, Meehl G A, Senior C A, Stevens B, Stouffer R J and Taylor K E 2016 Overview of the coupled model intercomparison project phase 6 (CMIP6) experimental design and organization *Geosci. Model Dev.* **9** 1937–58

Eyring V *et al* 2021 Human influence on the climate system *Climate Change 2021: The Physical Science Basis. Contribution of Working Group I to the Sixth Assessment Report of the Intergovernmental Panel on Climate Change* ed V Masson-Delmotte (Cambridge University Press) pp 423–552

Freeman E *et al* 2017 ICOADS Release 3.0: a major update to the historical marine climate record *Int. J. Climatol.* **37** 2211–32

Gleckler P J, Wigley T M L, Santer B D, Gregory J M, AchutaRao K and Taylor K E 2006 Krakatoa's signature persists in the ocean *Nature* **439** 675–675

Gregory J *et al* 2013 Climate models without preindustrial volcanic forcing underestimate historical ocean thermal expansion *Geophys. Res. Lett.* **40** 1600–4

Gulev S *et al* 2021 Changing state of the climate system *Climate Change 2021: The Physical Science Basis. Contribution of Working Group I to the Sixth Assessment Report of the Intergovernmental Panel on Climate Change* ed V Masson-Delmotte (Cambridge University Press) pp 287–422

Hardacre C, Mulcahy J P, Pope R J, Jones C G, Rumbold S T, Li C, Johnson C and Turnock S T 2021 Evaluation of SO_2, SO_4^{2-} and an updated SO_2 dry deposition parameterization in the United Kingdom Earth System Model *Atmos. Chem. Phys.* **21** 18465–97

Hawkins E *et al* 2017 Estimating changes in global temperature since the preindustrial period *Bull. Am. Meteorol. Soc.* **98** 1841–56

Hegerl G C *et al* 2019 Causes of climate change over the historical record *Environ. Res. Lett.* **14** 123006

Hegerl G C, Brönnimann S, Schurer A and Cowan T 2018 The early 20th century warming: Anomalies, causes and consequences *WIREs Clim. Change* **9** e522
Hoesly R M *et al* 2018 Historical (1750–2014) anthropogenic emissions of reactive gases and aerosols from the Community Emissions Data System (CEDS) *Geosci. Model Dev.* **11** 369–408
Hurtt G C *et al* 2020 Harmonization of global land use change and management for the period 850–2100 (LUH2) for CMIP6 *Geosci. Model Dev.* **13** 5425–64
Iwi A M, Hermanson L, Haines K and Sutton R T 2012 Mechanisms linking volcanic aerosols to the atlantic meridional overturning circulation *J. Clim.* **25** 3039–51
Jungclaus J H *et al* 2017 The PMIP4 contribution to CMIP6 - Part 3: the last millennium, scientific objective and experimental design for the PMIP4 *past1000* simulations *Geosci. Model Dev.* **10** 4005–33
Kageyama M *et al* 2018 The PMIP4 contribution to CMIP6 - Part 1: Overview and over-arching analysis plan *Geosci. Model Dev.* **11** 1033–57
Kaplan J O, Krumhardt K M and Zimmermann N 2009 The prehistoric and preindustrial deforestation of Europe *Quat. Sci. Rev.* **28** 3016–34
Kent E C and Kennedy J J 2021 Historical estimates of surface marine temperatures *Ann. Rev. Mar. Sci.* **13** 283–311
Lamarque J-F *et al* 2010 Historical (1850–2000) gridded anthropogenic and biomass burning emissions of reactive gases and aerosols: methodology and application *Atmos. Chem. Phys.* **10** 7017–39
Malhi Y 2018 Ancient deforestation in the green heart of Africa *Proc. Natl Acad. Sci.* **115** 3202–4
Marshall L R *et al* 2024 Last millennium volcanic forcing and climate response using SO_2 emissions *EGUsphere* **21** 1–39
Meinshausen M *et al* 2017 Historical greenhouse gas concentrations for climate modelling (CMIP6) *Geosci. Model Dev.* **10** 2057–116
Miller G H *et al* 2012 Abrupt onset of the Little Ice Age triggered by volcanism and sustained by sea-ice/ocean feedbacks *Geophys. Res. Lett.* **39** 68
Morice C P *et al* 2021 An updated assessment of near-surface temperature change from 1850: the HadCRUT5 data set *J. Geophys. Res. Atmos.* **126** e2019JD032361
Morice C P *et al* 2025 An observational record of global gridded near surface air temperature change over land and ocean from 1781 *Earth Syst. Sci. Data* **17** 7079–100
Mulcahy J P *et al* 2020 Description and evaluation of aerosol in UKESM1 and HadGEM3-GC3.1 CMIP6 historical simulations *Geosci. Model Dev.* **13** 6383–423
Mulcahy J P *et al* 2023 UKESM1.1: development and evaluation of an updated configuration of the UK Earth System Model *Geosci. Model Dev.* **16** 1569–600
Otto-Bliesner B L, Brady E C, Fasullo J, Jahn A, Landrum L, Stevenson S, Rosenbloom N, Mai A and Strand G 2016 Climate variability and change since 850 CE: an ensemble approach with the community earth system model *Bull. Am. Meteorol. Soc.* **97** 735–54
PAGES2K 2013 Continental-scale temperature variability during the past two millennia *Nat. Geosci.* **6** 339–46
Parker D E, Legg T P and Folland C K 1992 A new daily central England temperature series, 1772–1991 *Int. J. Climatol.* **12** 317–42
Pausata F S R *et al* 2015 Impacts of high-latitude volcanic eruptions on ENSO and AMOC *Proc. Natl Acad. Sci.* **112** 13784–8
Raible C C *et al* 2016 Tambora 1815 as a test case for high impact volcanic eruptions: earth system effects *WIREs Clim. Change* **7** 569–89
Schleussner C-F *et al* 2016 There are discernible differences in climate impacts between 1.5 °C and 2 °C of warming. The extent of countries' near-term mitigation ambition will determine the success of the paris agreement's temperature goal *Nat. Clim. Change* **6** 827–35
Schmidt G A *et al* 2012 Climate forcing reconstructions for use in PMIP simulations of the Last Millennium (v1.1) *Geosci. Model Dev.* **5** 185–91
Schurer A P *et al* 2013 Separating forced from chaotic climate variability over the past millennium *J. Clim.* **26** 6954–73
Schurer A P, Hegerl G C, Goosse H, Bollasina M A, England M H, Smith D M and Tett S F B 2023 Role of multi-decadal variability of the winter North Atlantic Oscillation on Northern Hemisphere climate *Environ. Res. Lett.* **18** 044046
Schurer A P, Mann M E, Hawkins E, Tett S F B and Hegerl G C 2017 Importance of the pre-industrial baseline for likelihood of exceeding Paris goals *Nat. Clim. Change* **7** 563–7
Schurer A P, Tett S F B and Hegerl G C 2014 Small influence of solar variability on climate over the past millennium *Nat. Geosci.* **7** 104–8
Sellar A A *et al* 2019 UKESM1: description and evaluation of the U.K. Earth system model *J. Adv. Modeling Earth Syst.* **11** 4513–58
Sellar A A *et al* 2020 Implementation of U.K. Earth system models for CMIP6 *J. Adv. Modeling Earth Syst.* **12** e2019MS001946
Sippel S *et al* 2024 Early-twentieth-century cold bias in ocean surface temperature observations *Nature* **635** 618–24
Swingedouw D, Mignot J, Ortega P, Khodri M, Menegoz M, Cassou C and Hanquiez V 2017 Impact of explosive volcanic eruptions on the main climate variability modes *Glob. Planet. Change* **150** 24–45
Taylor K E, Stouffer R J and Meehl G A 2012 An overview of CMIP5 and the experiment design *Bull. Am. Meteorol. Soc.* **93** 485–98
Tett S F B *et al* 2007 The impact of natural and anthropogenic forcings on climate and hydrology since 1550 *Clim. Dyn.* **28** 3–34
Toohey M and Sigl M 2017 Volcanic stratospheric sulfur injections and aerosol optical depth from 500 BCE to 1900 CE *Earth Syst. Sci. Data* **9** 809–31
Vieira L E A, Solanki S K, Krivova N A and Usoskin I 2011 Evolution of the solar irradiance during the Holocene *Astron. Astrophys.* **531** A6
Wallis E J, Osborn T J, Taylor M, Jones P D, Joshi M and Hawkins E 2024 Quantifying exposure biases in early instrumental land surface air temperature observations *Int. J. Climatol.* **44** 1611–35
Wu Y, Chi J and Kok L 2017 SATIRE-M reconstruction of spectral solar irradiance over the Holocene (https://doi.org/10.17617/3.11)
Zambri B, Robock A, Mills M J and Schmidt A 2019 Modeling the 1783–1784 laki eruption in Iceland: 1. Aerosol evolution and global stratospheric circulation impacts *J. Geophys. Res. Atmos.* **124** 6750–69
Zhang R *et al* 2019 A review of the role of the Atlantic meridional overturning circulation in Atlantic multidecadal variability and associated climate impacts *Rev. Geophys.* **57** 316–75